Structure Determination of a Key Intermediate of the Enantioselective Pd Complex Catalyzed Allylic Substitution Reaction

Jochen Junker,[a] Bernd Reif,[a, c] H. Steinhagen,[a, d] Bernd Junker,[a, e] I. C. Felli,[a, f] Michael Reggelin,[a, e] and Christian Griesinger*[a, b]

Dedicated to Prof. Dr. Horst Kessler on the occasion of his 60th birthday

Abstract: The structure of a catalytic intermediate with important implications for the interpretation of the stereochemical outcome of the palladium complex catalyzed allylic substitution with phosphino–oxazoline (PHOX) ligands is determined by liquid state NMR. The complex displays a novel structure that is highly distorted compared with other palladium η^2-olefin complexes known so far. The structure has been determined from nuclear overhauser data (NOE), scalar coupling constants, and long range projection angle restraints derived from dipole dipole cross-correlated relaxation of multiple quantum coherence. The latter restraints have been implemented into a distance geometry protocol. The projection angle restraints yield a higher precision in the determination of the relative orientation of the two molecular moieties and are essential to provide an exact structural definition of the olefinic part of the catalytic intermediate with respect to the ligand.

Keywords: catalysts · NMR spectroscopy · palladium · P ligands · reaction mechanisms

Introduction

Recently, the catalytic cycle of the Pd complex catalyzed allylic substitution reaction using sodium dimethyl malonate (NaDMM) as nucleophile (Scheme 1) has been elucidated by real time kinetic NMR spectroscopy.[1] The resting state of the reaction, the precursor η^3-complex **1**, could be described in detail by X-ray analysis as well as by NMR spectroscopy. It could be shown that cross-correlated relaxation of multiple quantum coherences provides accurate values for long range projection angles.[2, 7, 8, 9] Compound **2** is formed by nucleophilic attack of NaDMM onto the *exo*-diastereomer of the allyl complex **1**. The reaction occurs nearly exclusively from the *Re*-face and *trans* to phosphorus, of the allylic moiety giving rise to the uniformly configurated substitution product **2** which can be regarded as the primary Pd^0-product complex. However, despite some preliminary NMR work, the structure of the catalytic intermediate **2** remains unresolved.

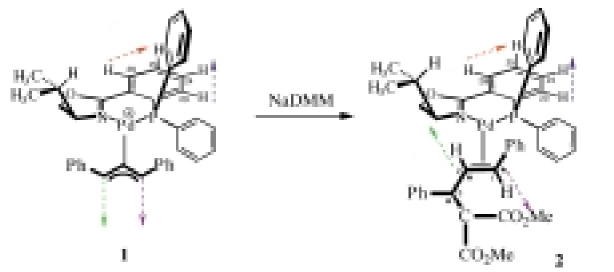

1 2

Scheme 1. Formation of complex **2** with sodium dimethyl malonate (NaDMM) as the nucleophile.

Results and Discussion

In this paper, we describe the structure determination of the metastable complex **2** which could not be crystallized so far. Its structure is unprecedented by comparison with all other

[a] Prof. Dr. C. Griesinger, Dipl.-Chem. J. Junker, Dr. B. Reif
Institut für Organische Chemie, Marie-Curie-Strasse 11
Universität Frankfurt, 60439 Frankfurt (Germany)
E-mail: cigr@krypton.org.chemie.uni-frankfurt.de

[b] Prof. Dr. C. Griesinger
also: Max Planck Institut für Biophysikalische Chemie
Am Faßberg, 37077 Göttingen (Germany)

[c] Dr. B. Reif
present address: Institut für Organische Chemie und Biochemie II
Technische Universität München, Lichtenbergstr. 4
85747 Garching (Germany)

[d] Dr. H. Steinhagen
present address: Bayer AG, Business Group Pharma
PH-R CR Medicinal Chemistry II, 42096 Wuppertal (Germany)

[e] Dipl.-Chem. B. Junker, Prof. Dr. M. Reggelin
present address: Institut für Organische Chemie
Universität Mainz, Duesbergweg 9–14, 55128 Mainz (Germany)
E-mail: re@cortex.chemie.uni-mainz.de

[f] Dr. I. C. Felli
present address: Center for Magnetic Resonance (CERM)
University of Florence, Via Luigi Sacconi 6
50019 Sesto Fiorentino, Firenze (Italy)

  0947-6539/00/0617-3281 $ 17.50+.50/0

known Pd-olefin complexes and shows large deviations from a planar pseudosymmetrical geometry. In this context, planarity refers to the fact that the atoms C1, C2, Pd, P, and N normally lie in a plane in these complexes. Pseudosymmetry refers to the fact that the olefin bond is orthogonal to the bisector of the N-Pd-P bond angle in most Pd-olefin complexes. For the description of the structure, we introduce the three angles ζ, ζ' (Figure 1), and ϕ.

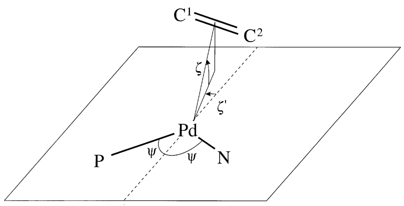

Figure 1. Definition of the angles ζ and ζ' for the description of the Pd olefin complexes. The angle ζ describes the rotation of the olefin out of the Pd-P-N plane while ζ' is the deviation from pseudosymmetry of the complex. The pseudotorsional angle ϕ (not shown) is measured between N-P-C^1-C^2.

While ζ describes the displacement of the center of mass of the C−C bond out of the Pd,P,N plane, ζ' is the rotation of the center of mass of the C−C bond around an axis perpendicular to the Pd-P-N plane away from the bisector of the N-Pd-P bond angle 2ψ. ϕ is the torsion angle formed by P,N,C^1, and C^2. The η^2-palladium olefin complex structures in the Cambridge Structural Data Base (CSD,[3] see Table 3) show little deviations of all ζ, ζ', ϕ from 0°. However, there is one example, GENJAK **3**,[4, 5] in which the olefin is covalently linked to the Pd ligand by a short linker in which $\zeta = 17°$ and $\zeta' = 17.7°$. This indicates a certain softness of the Pd potential with respect to rotations around these two angles. The only published structure of an olefin complex so far (NIBVOJ **4**)[6] in which the coordinating atoms connected to Pd are N and P displays an angle $\phi = -5.3°$; this demonstrates that deviations for ϕ are also possible.

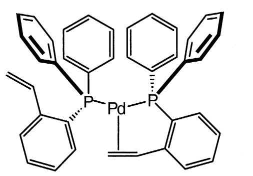

3

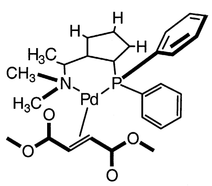

4

A NMR sample could be prepared containing about 75% of the phosphorus in the form of the Pd^0-olefin complex **2**. The assignment of the protons and the important carbons was achieved by 2D-NMR methods as described in ref. [1]. Two cross-correlated relaxation rates were measured between the H^{26},H^{25} vector and the C^2,H^2 vector as well as the H^{23},H^{24} vector and the C^2,H^2 vector using the pulse sequence already published.[7] The cross-correlated relaxation rates can be extracted from the submultiplets (Figure 2). Assuming the same correlation time for the η^2-olefin complex **2** and for the allyl compound **1**, the projection angles 48°/132° between H^2,C^2 and H^{25},H^{26} and 61°/119° between H^2,C^2 and H^{23},H^{24} could be derived (Table 1).

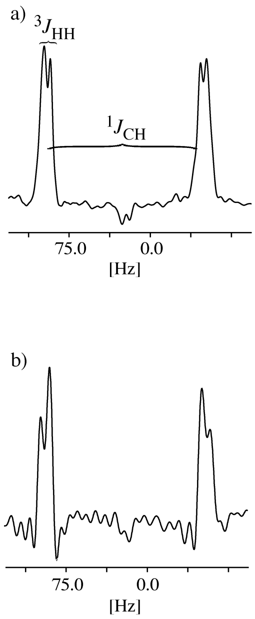

Figure 2. Experimental spectra of the real time DQ/ZQ-HPC correlation experiment for the olefinic palladium complex **2**. ω_1 traces are shown through the ZQ spectrum of the DQ/ZQ-HPC experiment of **2** at −60°C in [D$_8$]THF and a concentration of **2** of approximately 88mM. a) Correlation between H^{23} and C^2. b) Correlation between H^{26} and C^2. The signal is split due to the ^1J(C^2,H^2) and the ^3J(H^{26},H^{25}) for H^{26} b) and the ^3J(H^{23},H^{24}) scalar coupling for H^{23} a). The experimental parameters for the pulse sequence as described in [7] were the following: The C^2-selective ^{13}C BIRD pulse (^{13}C pulse of 2.75 ms duration) serves to refocus all homonuclear scalar couplings to C^1 and C^3, as well as long range heteronuclear scalar proton carbon couplings during the indirect evolution period. ($J_{C2,P}$ = 47 Hz; δ[C^1] = 60.7, δ[C^2] = 113.2, δ[C^3] = 101.7). The total duration between the first excitation pulse and the detection amounts to $1/J$(H,H) = 128.2 ms. $\Delta' = 46.0$ ms. Gradients serve to suppress pulse imperfections and artefacts (G_1 = 33 Gauss cm^{-1}). The experiment for H^{23} (H^{26}): number of scans: 32 (256), number of t_1 experiments: 224, spectral width in $\omega_1/2\pi$: 500 Hz. The total duration of the experiment amounts to 6.0 h (48.0 h).

From the high resolution X-ray crystal structure of **1**, we learned that the hydrogen atoms in the allylic moiety are not within the plane of the allylic carbons.[7] Therefore, we determined the projection angles of the neighboring HC vectors in the olefin moiety from cross-correlated relaxation rates $\Gamma^{c}_{C_iH_iC_jH_j}$ as well. It is obvious that such torsion angles, which describe the deviation of the olefin moiety from planarity, could not be determined from ^3J(H,H) coupling constants due to the lack of model compounds to yield a Karplus calibration for this kind of molecules.

For technical reasons, we used a *J*-resolved *Γ-HCCH* experiment instead of a *quantitative Γ-HCCH* experiment.[2b, 8] Figure 3 shows the pulse sequence, a real time H,C,C experiment in which H,C double- and zero-quantum coherences evolve during t_1.

In order to validate the method, the experiment was first applied to the allylic moiety of complex **1**, whose crystal

Table 1. Nuclear assemblies, cross-correlated relaxation rates (Γ^c) and projection angles (θ) for compounds **1** and **2**.

Nuclei	Γ^c/θ	Compound **1**	Compound **2**
(H^{25}H^{26},C^{3}H^3)	Γ^c [Hz]	+0.33 ± 0.30	+0.8 ± 0.30
	θ^{NMR} [°]	θ_1 = 52, 128, ±3	θ_1 = 48, 132, ±3
	$\theta^{X\text{-}ray}$ [°]	54	–
(H^{23}H^{24},C^{3}H^3)	Γ^c [Hz]	+1.60 ± 0.10	−0.6 ± 0.1
	θ^{NMR} [°]	θ_2 = 41, 139, ±1	θ_2 = 61, 119, ±1
	$\theta^{X\text{-}ray}$ [°]	140	–
(H^{2}C^2,C^{1}H^1)	Γ^c [Hz]	11.20 ± 0.60	3.5 ± 1.0
	θ^{NMR} [°]	–	(45° ± 3)
	$\theta^{X\text{-}ray}$ [°]	158.4	–
(H^{2}C^2,C^{3}H^3)	Γ^c [Hz]	13.67 ± 0.72	n/a[a]
	$\theta^{X\text{-}ray}$ [°]	168.7	–

[a] Not analyzed.

0947-6539/00/0617-3282 $ 17.50+.50/0 *Chem. Eur. J.* **2000**, *6*, No. 17

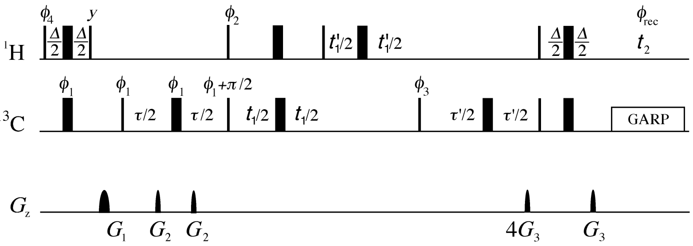

Figure 3. Real time DQ/ZQ-HCC correlation experiment. Coherence transfer is accomplished via an INEPT H,C transfer and a C,C-COSY transfer. Narrow and thick bars represent 90° and 180° pulses, respectively. The default phase for pulses, unless otherwise indicated, is x. The phases ϕ_1 and ϕ_2 are shifted by 90° in subsequent free induction decays (FIDs) and stored separately to differentiate between double- and zero-quantum coherences. Coaddition and substraction of the FIDs yields the zero- and double-quantum spectrum, respectively. Quadrature detection in the indirect dimension for both double-and zero-quantum evolution time is achieved by incrementation of ϕ_1 in subsequent FIDs according to States TPPI. In the indirect dimension, increments for t_1 and t_1' were set differently to yield the optimal resolution of the multiplet components. For the allyl (olefin) complex, the increments for t_1 and t_1' are set to 220.96 μs (100.0 μs) and 55.24 μs (100.0 μs), respectively. In both cases, 88 increments (16 scans per increment) were coadded to yield a total experimental time of 3.8 h. Delays were set to yield optimal transfer efficiency with $\Delta = ½J_{CH} =$ 3.4 ms and $\tau = ½J_{CC} = 10$ ms. Gradient values are given in percent of the maximum gradient strength $G_1 = 37$, $G_2 = 13$, $G_3 = 13$, $G_4 = 80$, $G_5 = 20$. G_4 and G_5 serve to suppress artefacts. The phase cycle is given by $\phi_4 = x, -x$; $\phi_2 = 2(x), 2(-x)$; $\phi_1 = 4(x), 4(-x)$; $\phi_3 = 8(x), 8(-x)$; $\phi^{rec} = x, -x, -x, x, -x, x, x, -x$.

structure is known, and then to the olefin complex **2**. Two cross-correlated relaxation rates were measured between the C^2-H^2 bond vector with both the C^1-H^1 and the C^3-H^3 bond vector for complex **1**. Regarding the evolution of cross-correlated relaxation rates, care is taken to refocus cross-correlated relaxation between chemical shift anisotropy and dipolar couplings.[9] The pulse sequence is optimized for transfer from a carbon with a single carbon coupling partner by setting $\tau = 1/(2J_{CC})$. Therefore, only double- (DQC) and zero-quantum coherences (ZQC) between H^1 and C^2 as well as between H^3 and C^2 are excited. The multiplet structure of the H^1,C^2 double-quantum coherence is a doublet of doublets of doublets due to the couplings to C^1 (^1J(C^1,H^1) $\pm$ ^1J(C^1,C^2)), to H^2 (^1J(H^2,C^2) $\pm$ ^3J(H^2,H^1)), and to C^3 (^1J(C^3,C^2) $\pm$ ^3J(C^3,H^1)). The respective spin states of the multiplet according to the couplings to C^1, H^2, and C^3 are denoted as $\alpha\alpha\alpha$, $\alpha\alpha\beta$, $\alpha\beta\alpha$ etc. as depicted in Figure 4. For values of the chemical shifts of these resonances and the size of the involved scalar couplings see ref. [10].

Extraction of the $\Gamma^c_{C_iH_iC_jH_j}$ rates can be performed as previously described[7] by analyzing the $\alpha\alpha\alpha$ and $\alpha\beta\alpha$, as well as the $\beta\beta\beta$ and $\beta\alpha\beta$ components of the multiplet which differ in relaxation by the following rates:

$$\Gamma^c_{\alpha\alpha\alpha} - \Gamma^c_{\alpha\beta\alpha} = \Gamma^c_{\beta\beta\beta} - \Gamma^c_{\beta\alpha\beta} = 2\Gamma^c_{C_1H_1C_2H_2} + 2\Gamma^c_{C_2C_1C_2H_2} + 2\Gamma^c_{C_2H_2C_2C_3} \quad (1)$$

All rates except for $\Gamma^c_{C_iH_iC_jH_j}$ are extremely small and were therefore neglected. The cross-correlated relaxation rate can be translated into the projection angle according to:

$$\Gamma^c_{C_iH_iC_jH_j} = \frac{\gamma_{^1H}\gamma_{^{13}C}}{(r_{C_iH_i})^3 (r_{C_jH_j})^3}\left(\frac{\hbar\mu_0}{4\pi}\right)^2 P_2(\cos\theta_{C_iH_i,C_jH_j})J(0) \quad (2)$$

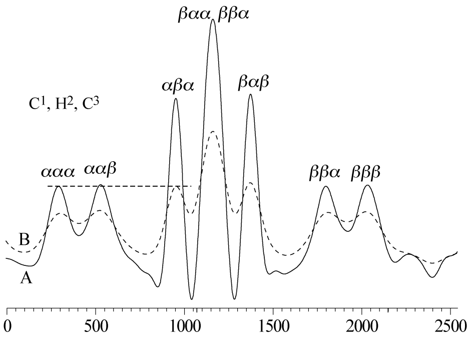

Figure 4. Traces along the ^{13}C dimension of the $4H_1{}^+C_{1z}C_2{}^+$ multiplet of compound **1** in the HCC-DQ/ZQ experiment. The full line (A) is the trace extracted from the 2D experiment. The splittings due to the various couplings are indicated. They are due to the C^1: ^1J(C^1,C^2)+^1J(H^1,C^1), H^2: ^1J(H^2,C^2)+^{3}J(H^1,H^2), and the C^3: ^1J(C^2,C^3)+^3J(C^3,H^1). The line intensities of the $\alpha\alpha\alpha$ (meaning $C^1_\alpha H^2_\alpha C^3_\alpha$) with respect to the $\alpha\beta\alpha$ line and the $\beta\beta\beta$ with respect to the $\beta\alpha\beta$ line reflect the desired HCCH cross-correlated relaxation rate as indicated in Equation (1). The dotted line (B) represents the trace A after convolution with the appropriate line broadening such that the intensities of the $\alpha\alpha\alpha$ ($\beta\beta\beta$) line of A matches that of the $\alpha\beta\alpha$ ($\beta\alpha\beta$) line of B.

where P_2 indicates the second order Legendre polynomial. We determined Γ(H^{2}C^2,C^{3}H^3) = 13.67 $\pm$ 0.72 Hz and Γ(H^{2}C^2, C^{1}H^1) = 11.20 $\pm$ 0.60 Hz for the allyl complex **1** by using the same fitting routine as described in ref. [7]. The ratio of these two rates Γ(H^{2}C^2,C^{3}H^3)/Γ(H^{2}C^2,C^{1}H^1) = 1.22 is in excellent agreement with the ratio of P_2(cosθ(H^{2}C^2,C^{3}H^3))/ P_2(cosθ(H^{2}C^2, C^{1}H^1)) = 1.18[11] as found from the X-ray structure with θ(H^{2}C^2,C^{3}H^3) = 168.7° and θ(H^{2}C^2, C^{1}H^1) = 158.4°. The experimental results are summarized in Table 1.

For the olefin complex **2**, strong coupling between C^1 and C^2 has to been taken into account rendering the intensities of each individual submultiplet line of the observed DQC between H^1 and C^2 differently even without cross-correlated relaxation. Therefore the multiplet pattern, which would be expected without cross-correlated relaxation but including strong coupling effects, has been simulated as a reference multiplet (dashed line in Figure 5).

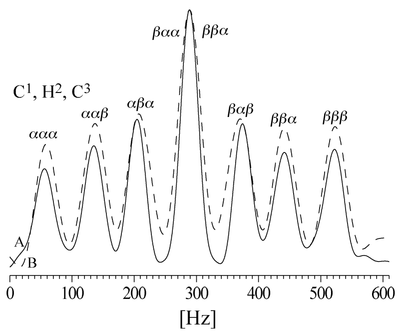

Figure 5. Experimental (full line A) and simulated data (dotted line B) for compound **2** recorded with the HCC-DQ/ZQ experiment of Figure 3. The Figure shows a 1D trace along the ^{13}C dimension of the signal resulting from the coherence $4H_1{}^+C_{1z}C_2{}^+$. The splittings due to the various couplings are indicated. They are due to the C^1: ^1J(C^1,C^2)+^1J(H^1,C^1), H^2: ^1J(H^2,C^2)+^{3}J(H^1,H^2), and the C^3: ^1J(C^2,C^3)+^3J(C^3,H^1). The values used in the simulation were according to ref. [10] In the simulation (B), the effect of strong couplings, but not of cross-correlated relaxation is taken into account. Note the different line intensities due to the strong coupling between C^1 and C^2. The result of the fitting of trace B to trace A including cross-correlated relaxation is not shown here.

The experimental trace along the ^{13}C dimension of the signal resulting from the $4H_1^+C_{1z}C_2^+$ coherence (DQC between H[1] and C[2]) for the olefin complex is given as a full line in Figure 5. Taking into account the intensities of the submultiplet affected by strong coupling, we find for $\Gamma(\mathrm{H^2C^2,C^1H^1}) = 3.5 \pm 1$ Hz which translates into a projection angle $\theta(\mathrm{H^2C^2,C^1H^1}) = 45 \pm 3^\circ$ (or $135 \pm 3^\circ$) when using the Γ(HC,HC) cross-correlated relaxation rates of the allyl fragment as reference.

The standard DG/DADD protocol consists of four steps. 1) Generation of the structures in 4D space based on the distances (distance geometry in *metrize*). 2) Optimization of the geometry by including the chiral restraints, maintaining the distances, in four-dimensional space (distance and angle driven dynamics in 4D), by using a simplified force field based on all restraints, first conjugate gradients (*optimize*), and then a Monte Carlo search (*shake*) further improve the geometry. 3) Projection of the 4D coordinates into 3D space (*dimred*). 4) Distance and angle driven dynamics in 3D.

The two long range (θ_1 and θ_2 of **2**, Table 1) and the one short range projection angle restraint (θ_3 of **2**, Table 1) have been incorporated into a distance geometry (DG) calculation[12] which consists of the the four steps described above. The additional potentials and forces are given in Equation (5) and (7) and were incorporated into the 4D and 3D DAAD programs, exploiting their formal similarity to the chiral volume.

$$V^{\mathrm{c}}_{\mathrm{A^1A^2,B^1B^2}} = k[\Gamma^{\mathrm{c,theo}}(\theta_{\mathrm{A^1A^2,B^1B^2}}) - \Gamma^{\mathrm{c,exp}}_{\mathrm{A^1A^2,B^1B^2}}]^2 = k\left[\frac{\kappa}{r_{\mathrm{A}}^2 r_{\mathrm{B}}^2}\left\{3\left(\vec{A}\vec{B}\right)^2 - \left(\vec{A}\right)^2\left(\vec{A}\right)^2\right\} - \Gamma^{\mathrm{c,exp}}_{\mathrm{A^1A^2,B^1B^2}}\right]^2 \quad (5)$$

with:

$$\kappa = \frac{\gamma_{\mathrm{A^1}}\gamma_{\mathrm{A^2}}}{(r_{\mathrm{A}})^3}\frac{\gamma_{\mathrm{B^1}}\gamma_{\mathrm{B^2}}}{(r_{\mathrm{b}})^3}\left(\frac{\hbar\mu_0}{4\pi}\right)^2 J(0) \quad \text{and} \quad \vec{A} = \vec{A}^1 - \vec{A}^2, \vec{B} = \vec{B}^1 - \vec{B}^2 \quad (6)$$

The forces for each of the involved atoms $X = [\mathrm{A^1, A^2, B^1, B^2}]$ are calculated from:

$$\vec{F}_{\mathrm{X}} = -\vec{\nabla}_{\mathrm{X}} V^{\mathrm{c}}_{\mathrm{A^1A^2,B^1B^2}} \quad (7)$$

For the forces, the distances r_{A} and r_{B} are assumed to be constant since they are fixed by the holonomic distance constraints. Although the forces according to Equation (7) are not perpendicular to the two vectors $\vec{A}$ and $\vec{B}$ we rely on the holonomic restraints to maintain the bond lengths. The force constant for the distance restraints is set to 1 in the program, the force constants for the chiral and projection angle restraints (k) were found to be optimal with 80 and 15, respectively.

In addition to the NOE data, scalar couplings and cross-correlated relaxation rates, the Pd–C[1] and Pd–C[2] distances were restrained to 2–2.5 Å according to X-ray structures of Pd-olefin complexes extracted from the CSD. This proved to be necessary since structures without this restraint had Pd–C[1] and Pd–C[2] distances of 4–5 Å after the DG/DADD calculation.

The 20 structures generated by DG/DADD using only NOE-derived distance data as experimental restraints with the lowest violations of these are superimposed in Figure 6.

Averages of selected structural parameters are compiled in Table 2. As shown in Figure 6 the position of the double bond is not very well defined. In contrast to that the superposition of the 20 structures generated by DG/DADD including the projection angle restraints with lowest violations of restraints result in a dramatically improved convergence (Figure 7). The precision of the position of the olefinic bond as well as that of the two phenyl rings attached to this moiety has improved (Table 2).

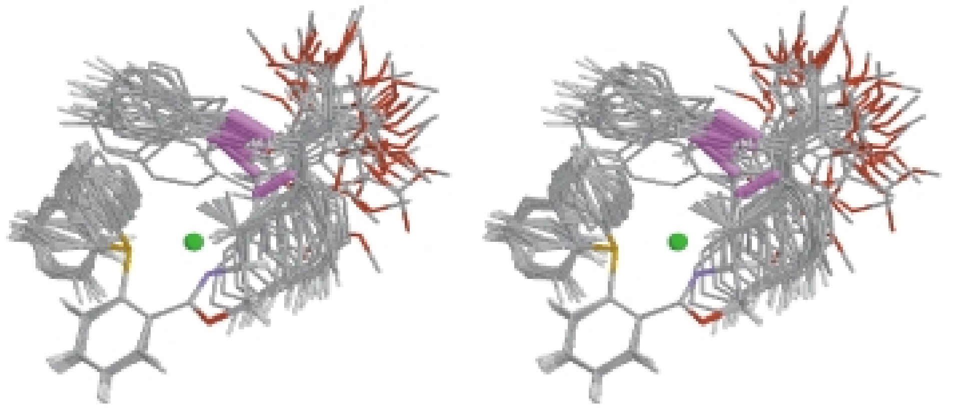

Figure 6. Superposition of the aromatic part of the ligand of the 20 best structures generated by DG/DADD using experimental NOE data and the Pd/C[1] and Pd/C[2] restraints. The position of the olefinic bond (purple) is not well defined.

There are no violations of the experimental restraints in these structures. The structure family is characterized by $\zeta = 45^\circ$ and $\zeta' = 19^\circ$ (for a definition of these angles see Figure 1). The resulting N/P–C[1]/C[2] pseudo dihedral angle is given as $\phi = -3.2 \pm 0.9^\circ$. Omitting the distance restraints that are between pseudoatoms only, we obtain a slightly different structure family with $\zeta = 31^\circ$ and $\zeta' = 20^\circ$. Thus, the deviation from planarity (ζ) is not very accurately defined. However, the deviation from pseudosymmetry (ζ') is. It can be inferred from Table 2 that the overall geometry of the complex is determined by the NOEs. The cross-correlated relaxation rates restrict the space of conformations further and therefore refine the structure.

It is interesting to know how the atoms move when the nucleophile attacks the allyl complex **1**. This can be evaluated by calculating the angles ζ, ζ', and ϕ as well for the C[1]–C[2] olefin moiety in this complex. We calculate $\zeta = 1^\circ$ and $\zeta' = 16.5^\circ$ and $\phi = -11.9^\circ$. This suggests that atoms C[1]–C[2] are moving out of the plane (ζ motion), while there is almost no motion about the axis perpendicular to the plane (ζ' motion) and little change of the pseudodihedral angle ϕ. Thus, the

0947-6539/00/0617-3284 $ 17.50+.50/0 *Chem. Eur. J.* **2000**, *6*, No. 17

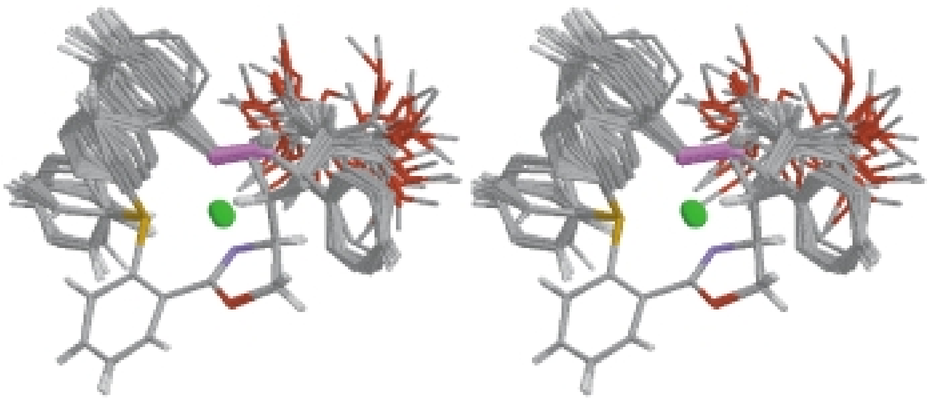

Figure 7. Superposition of the aromatic part of the ligand of the 20 best structures generated by DG/DADD using NOE data, the Pd/C[1] and Pd/C[2] restraints, and projection angle restraints. With the additional information the position of the olefinic bond (purple) becomes well defined.

Table 2. Characteristic distances and angles for **2** from the structure calculations and the cross-correlated relaxation experiments.

Structural parameter	Method 1[a]	Method 2[b]	Method 3[c]	CCR[d]
θ($H^{23}H^{24}$,C^2H^2) [Hz]	97.2 ± 9.3	110.7 ± 1.5	115.1 ± 0.5	119.0 ± 1.0
θ($H^{25}H^{26}$,C^2H^2) [Hz]	43.7 ± 13.8	33.2 ± 1.4	41.1 ± 1.2	48.0 ± 3.0
θ(C^1H^1,C^2H^2) [Hz]	16.8 ± 8.5	40.4 ± 0.5	44.8 ± 0.4	45.0 ± 3.0
r(Pd,C^1) [Å]	2.18 ± 0.1	2.05 ± 0.01	2.06 ± 0.01	–
r(Pd,C^2) [Å]	2.45 ± 0.1	2.52 ± 0.001	2.33 ± 0.005	–
ζ [°]	41.0 ± 12.4	45.13 ± 3.8	31.9 ± 2.35	–
ζ' [°]	17.70 ± 4.2	17.80 ± 3.4	17.7 ± 3.2	–
NP,C^1C^2 [°]	-4.7 ± 10.4	-3.6 ± 1.6	-6.0 ± 0.5	–
Total error [kcal mol]$^{-1}$	13.1 ± 1.3	10.9 ± 0.25	5.9 ± 0.1	–

[a] DG calculation using only but all NOE data. [b] DG calculation with all NOE data and projection angle restraints. [c] DG calculation using projection angle restraints and NOEs excluding pseudoatom/pseudoatom distances. [d] Angles from the cross-correlated relaxation experiment.

nucleophilic attack of NaDMM onto the *Re*-face of C^3 in **1** follows a least-motion principle.

A comparison of the η^2-complex **2** with all other Pd-η^2-complexes found in the CSD, specially **3** and **4**, shows that the latter ones rarely deviate from planarity ($\zeta = 0°$, Figure 8). Obviously the maximum stability of Pd-η^2-olefin complexes is associated with ζ and ζ' angles being close to zero and any significant deviation of these two angles from that value may destabilize the complex. In the context of the catalytic cycle the minimal motion during nucleophilic attack and the destabilizing distortion of the coordination geometry in the primarily formed product complex **2** apparently favors product release which in turn is beneficial to the efficiency of the reaction.

Conclusion

We have determined the structure of the primarily formed product complex in the palladium complex catalyzed allylic substitution reaction using chiral phosphino – oxazoline ligands. The measurement of cross-correlated relaxation rates of molecular moieties across the Pd and their incorporation into DG calculations in conjunction with NOEs and coupling constants allows for a precise structural characterization. As a result a coordination sphere of the Pd in this complex was found that deviates largely from olefin complexes whose X-ray structures have been deposited so far. The most striking structural feature is the pronounced deviation of the olefinic moiety from the coordination plane. In addition, the pseudosymmetry, which is observed in other Pd olefin complexes, is disturbed in complex **2**. The olefin structure **2** can be related to the allylic structure from which it originates after nucleophilic attack by minimizing the motion of atoms in the reaction. This, together with a destabilization of the product complex as a consequence of the observed distortion of the coordination geometry, may be a reason of the efficiency of the catalyst.

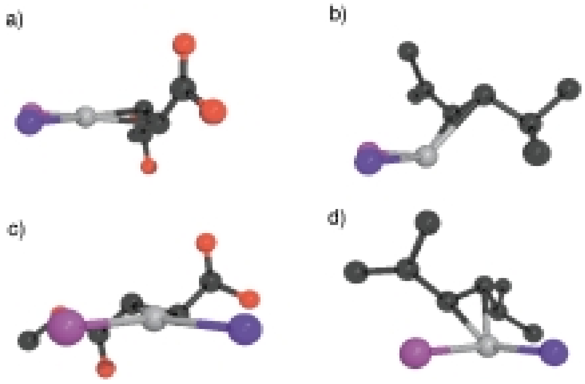

Figure 8. a) Partial structure of NIBVOJ (**4**) viewed along the N−P vector. The almost complete coplanarity of the olefinic carbons and the Pd,N,P atoms corresponding to a ζ-value close to zero is clearly visible. b) Partial structure of a representative member of the low energy family of the DG-calculated structures of **2**. The center of mass of the C=C double bond is out of the N-Pd-P plane by about $\zeta = 45.9°$. c) A small ζ'-value ($\zeta' = -2.44°$) describes the almost perfect orthogonality of the olefinic bond to the bisector of the N-Pd-P bond angle. d) In the calculated structure of **2** a view along this bisector illustrates the large deviation of this structural aspect ($\zeta' = 18.1°$) from typical Pd-olefin complexes.

Acknowledgement

Support by the Fonds der Chemischen Industrie and the DFG (B.J. and B.R.) is gratefully acknowledged. H.S. is indebted to Prof. G. Helmchen, University Heidelberg, for support. I.C.F. thanks the Alexander von Humboldt Foundation for a post-doctoral fellowship. The crystal structure of **1** has been determined by Dr. F. Rominger, University Heidelberg. Continuous support by Dr. W. Bermel and Dr. T. Keller, Bruker Rheinstetten, is gratefully acknowledged. All measurements have been done at the "Large-Scale Facility for Biomolecular NMR at the University of Frankfurt".

[1] H. Steinhagen, M. Reggelin, G. Helmchen, *Angew. Chem.* **1997**, *109*, 2199; *Angew. Chem. Int. Ed. Engl.* **1997**, *36*, 2108.

Table 3. Comparison of structural properties of **1** and **2** with known η^2-palladium olefin complexes.

Complex[a]	ζ [°]	ζ' [°]	ϕ [°]	d (Pd–C[1]) [Å]	d (Pd–C[2]) [Å]
1[b]	1.04	16.45	−11.92	2.2	2.3
2[c]	45.13	17.80	−3.60	2.5	2.2
2[d]	31.90	17.70	−6.01	2.3	2.1
Known η^2-palladium olefin complexes from the CSD file					
3 (GENJAK)[4]	17.04	17.69	−6.62	2.2	2.1
4 (NIBVOJ)[6]	0.59	−2.45	−5.25	2.1	2.1
ALETPD[13]	−3.15	−1.27	−3.38	2.1	2.1
BPBZAP[14]	1.27	5.31	−6.51	2.1	2.1
CARJOU[15]	0.60	−4.04	−1.19	2.2	2.1
FICBIC[16]	−2.27	−0.08	−2.18	2.1	2.1
HADSIO[17]	4.94	1.79	−1.50	2.1	2.1
HEDHAZ[18]	2.93	3.07	−1.74	2.1	2.1
LEZWES[19]	3.29	0.39	−1.05	2.2	2.1
SOLTAO[20]	1.96	−0.66	−0.45	2.1	2.2
VUFNUF[21]	1.49	−1.46	0.00	2.0	2.1
WEDFOA[22]	−3.29	8.39	−0.06	2.1	2.1
YEJDAS[23]	2.95	1.82	−1.53	2.1	2.1
YIZHIY[24]	2.19	0.76	−1.62	2.1	2.2
YIZHOE[25]	−0.46	−6.33	−1.70	2.2	2.1
ZAGHIY[26]	4.09	2.61	−7.31	2.1	2.1

[a] Capital letters refer to the ref-code of the Cambridge Structural Database (CSD). [b] Extracted from x-ray data.[7] [c] Calculated structure using all NOEs, coupling restraints and projection angle restraints. [d] Calculated strucutre neglecting pseudoatom-pseudoatom NOEs.

[2] a) B. Reif, M. Hennig, C. Griesinger, *Science* **1997**, *276*, 1230; b) T. Carlomagno, I. C. Felli, M. Czech, R. Fischer, M. Sprinzl, C. Griesinger, *J. Am. Chem. Soc.* **1999**, *121*, 1945; c) M. J. J. Blommers, W. Stark, C. E. Jones, D. Head, C. E. Owen, W. Jahnke, *J. Am. Chem. Soc.* **1999**, *121*, 1949; d) C. Griesinger, M. Hennig, J. P. Marino, B. Reif, H. Schwalbe, *Biol. Magn. Reson.* **1999**, 16, 259–367.

[3] The Cambridge Structural Database (CSD) is a property of the Cambridge Crystallographic Data Centre (CCDC), 12 Union Road, Cambridge CB2 1EZ, UK.

[4] Structures in the CSD are encoded by six capital letters.

[5] M. A. Bennett, C. Chiraratvatana, G. B. Robertson, U. Tooptakong, *Organometallics* **1988**, *7*, 1403.

[6] R. Fernandez-Galan, F. A. Jalon, B. R. Manzano, J. Rodriguez de la Fuente, M. Vrahami, B. Jedlicka, W. Weissensteiner, *Organometallics* **1997**, *16*, 3758.

[7] B. Reif, H. Steinhagen, B. Junker, M. Reggelin, C. Griesinger, *Angew. Chem.* **1998**, *110*, 2006–2009; *Angew. Chem. Int. Ed.* **1998**, *37*, 1903–1906.

[8] I. C. Felli, C. Richter, C. Griesinger, H. Schwalbe, *J. Am. Chem. Soc.* **1998**, *121*, 1956.

[9] B. Reif, A. Diener, M. Hennig, M. Maurer, C. Griesinger, *J. Magn. Reson.* **2000**, *143*, 45.

[10] $J(C^1,H^1) = 148.6$ Hz, $J(C^2,H^2) = 147.0$ Hz, $J(C^3,H^3) = 133.0$ Hz, $J(C^1,C^2) = 48.5$ Hz, $J(C^2,C^3) = 42.0$ Hz, $J(H^1,H^2) = 8.9$ Hz, $J(H^2,H^3) = 13.0$ Hz, $J(H^1,C^3) = 2$ Hz, $J(H^3,C^1) = 6.0$ Hz, $\Omega(C^1)/2\pi = -874.4$ Hz, $\Omega(C^2)/2\pi = -572.2$ Hz, $\Omega(C^3)/2\pi = 405.7$ Hz, $\Omega(H^1)/2\pi = -320.0$ Hz, $\Omega(H^2)/2\pi = 298.0$ Hz, $\Omega(H^3)/2\pi = 182.0$ Hz.

[11] As Γ is a rate, we have to transform the angular information obtained from the X-ray structure into a rate for the comparison. This is done using $P_2(x) = (3x^2 - 1)$.

[12] G. M. Crippen, T. F. Havel, *Distance Geometry and Molecular Conformation*, Research Studies Press, Somerset, **1988**.

[13] K. Okamoto, G. Kai, N. Yasuoka, N. Kasai, *J. Organomet. Chem.* **1974**, *65*, 427.

[14] C. G. Pierpont, P. M. Buchanan, H. H. Downs, *J. Organomet. Chem.* **1977**, *124*, 103.

[15] H. Werner, G. T. Crisp, P. W. Jolly, H.-J. Kraus, C. Krüger, *Organometallics* **1983**, *2*, 136.

[16] M. Hodgson, D. Parker, R. J. Taylor, G. Ferguson, *Organometallics* **1988**, *7*, 1761.

[17] V. V. Bashilov, P. V. Petrovskii, V. I. Sokolov, S. V. Lindeman, I. A. Guzey, Y. T. Struchkov, *Organometallics* **1993**, *23*, 991.

[18] R. von Asselt, C. J. Elsevier, W. J. J. Smeets, *Inorg. Chem.* **1994**, *33*, 1521.

[19] M. Murakami, T. Yoshida, Y. Ito, *Organometallics* **1994**, *13*, 2900.

[20] R. Benn, P. Betz, R. Goddard, P. W. Jolly, N. Kokel, C. Krüger, I. Topalovic, *Z. Naturforsch. Teil B* **1991**, *46*, 1395.

[21] V. P. Zagorodnikov, S. B. Katser, N. N. Vargaftik, M. A. Porai-Koshits, I. I. Moiseev, *Koord. Khim.* **1989**, *15*, 1540.

[22] W. A. Herrmann, W. R. Thiel, C. Brossmer, K. Ofele, T. Priermeier, W. Scherer, *J. Organomet. Chem.* **1993**, *461*, 51.

[23] F. Ozawa, M. Sugawara, T. Hayshi, *Organometallics* **1994**, *13*, 3237.

[24] R. Goddard, G. Hopp, P. W. Jolly, C. Krüger, R. Mynott, C. Wirtz, *J. Organomet. Chem.* **1995**, *486*, 163.

[25] J. Fawsett, R. D. W. Kemmitt, D. R. Russell, O. Serindag, *J. Organomet. Chem.* **1995**, *486*, 171.

[26] M. Murakami, T. Yoshiday, S. Kawanami, Y. Ito, *J. Am. Chem. Soc.* **1995**, *117*, 6408.

Received: March 3, 2000 [F2338]